

UA-Track: Uncertainty-Aware End-to-End 3D Multi-Object Tracking

Lijun Zhou^{1*}, Tao Tang^{2,1*}, Pengkun Hao¹, Zihang He¹, Kalok Ho¹, Shuo Gu¹,
Wenbo Hou¹, Zhihui Hao¹, Haiyang Sun¹, Kun Zhan¹, Peng Jia¹, Xianpeng Lang¹,
and Xiaodan Liang^{2†}

zhoulijun@lixiang.com, trent.tangtao@gmail.com

¹ Li Auto Inc.

² Shenzhen Campus of Sun Yat-sen University

<https://liautoad.github.io/ua-track-website/>



Fig. 1: The uncertainty issue in 3D multiple object tracking. The uncertainty issue refers to the models that do not provide accurate certainty estimates. In complex driving scenarios, the uncertainty issue arises from various factors, especially the occlusions and small size of target objects, which present significant challenges to achieving accurate tracking. The previous state-of-the-art end-to-end tracker, PF-Track [35], lacking uncertainty modeling, fails to track objects in certain complex scenarios.

Abstract. 3D multiple object tracking (MOT) plays a crucial role in autonomous driving perception. Recent end-to-end query-based trackers simultaneously detect and track objects, which have shown promising potential for the 3D MOT task. However, existing methods overlook the *uncertainty* issue, which refers to the lack of precise confidence about the state and location of tracked objects. Uncertainty arises owing to various factors during camera observation, especially occlusions and the small size of target objects, resulting in an inaccurate estimation of the object’s position, label, and identity. To this end, we propose an **Uncertainty-Aware** 3D MOT framework, UA-Track, which tackles the uncertainty problem from multiple aspects. Specifically, we first introduce an Uncertainty-aware Probabilistic Decoder to capture the uncertainty in object prediction with probabilistic attention. Secondly, we propose an Uncertainty-guided Query Denoising strategy to enhance training robustness and convergence against uncertainty. We also utilize

* Co-first author.

† Corresponding author.

Uncertainty-reduced Query Initialization, which leverages predicted 2D object location and depth information to reduce query uncertainty. As a result, our UA-Track achieves state-of-the-art performance on nuScenes benchmark, i.e., 66.3% AMOTA on test split, surpassing the previous best end-to-end solution by a significant margin of 8.9% AMOTA.

Keywords: UA-Track · Uncertainty-Aware · 3D Multi-Object Tracking

1 Introduction

3D multiple object tracking (MOT) [6, 22, 23, 35, 40, 44, 52] is an essential component for the perception of autonomous driving systems. The ability to accurately and robustly track objects in dynamic environments is crucial for ensuring smooth and safe navigation and reasonable decision-making. Traditional 3D MOT methods [4, 36, 49, 50, 52, 53, 57] rely on detector outcomes followed by a post-processing module like data association and trajectory filtering, leading to a complex pipeline. To avoid human-crafted heuristic design in detection-based trackers, recent advancements in end-to-end query-based approaches have shown promising potential in addressing the 3D MOT task by simultaneously detecting and tracking objects [6, 23, 35, 54, 55]. These methods have demonstrated impressive results in terms of tracking performance and efficiency. However, they assume the surrounding information is fully obtained and overlook the *uncertainty issue* that would often be encountered in 3D MOT. As shown in Fig. 1, the previous state-of-the-art end-to-end tracker, PF-Track [35], lacking uncertainty modeling, fails to track the objects in complex scenarios with uncertainty issues.

Although the uncertainty issue, which refers to neural networks that do not deliver certainty estimates or suffer from under-confidence, has been recognized in certain fields [11, 13, 42, 47, 51], e.g., action recognition [13] and camouflaged object detection [51], it has not been discussed or explored in the context of 3D MOT. Due to the complex environment of driving scenarios and the unique characteristics of tracking tasks, the uncertainty issue in 3D MOT is particularly challenging, and previous solutions for other specific domains cannot be directly applied here. In driving scenarios, the environment could be highly complex, often when driving in cities, with numerous objects such as vehicles and pedestrians interleaving across the scene, and exhibiting substantial variations in their motion patterns. Furthermore, tracked objects often cover a wide spatial tracking range and a long temporal tracking sequence. As a result, occlusion situations and the small size of target objects, frequently occur, which usually leads to some undetected or occluded objects losing track. These uncertainty factors present significant challenges to achieving accurate and robust 3D MOT.

In this paper, we propose an uncertainty-aware 3D MOT framework, UA-Track, to tackle the uncertainty problem from multiple aspects. Firstly, we introduce an Uncertainty-aware Probabilistic Decoder to capture and model the uncertainty during object prediction. Specifically, we model attention scores as Gaussian distributions instead of deterministic outputs, to quantify the predictive uncertainty. Secondly, we propose an Uncertainty-guided Query Denoising

strategy to further improve the training process. During the training stage, we add noises to ground-truth bounding boxes to form noised queries and selectively denoise queries based on their uncertainty levels, enhancing the robustness and convergence against uncertainty of training procedure. Moreover, we present the Uncertainty-reduced Query Initialization module, which leverages predicted 2D object location and depth information to bootstrap latent query states of the objects with reduced uncertainty during the query initialization stage. By incorporating learned certain priors, we enhance the accuracy of initial object localization, leading to more reliable tracking results. Experimental results on the nuScenes benchmark demonstrate the effectiveness of our UA-Track framework. It achieves state-of-the-art performance with an impressive 66.3% AMOTA on the test split, surpassing the previous best end-to-end solution by a significant margin of 8.9% AMOTA. These results highlight the importance of addressing the uncertainty issue in 3D MOT and showcase the potential of our uncertainty-aware framework in advancing the field of autonomous driving perception.

To summarize, our contributions are as follows:

- We notice the uncertainty issue in 3D MOT, especially the occlusions and small size of target objects, and propose an uncertainty-aware framework, UA-Track, for 3D MOT.
- We propose three well-designed modules, the Uncertainty-aware Probabilistic Decoder, Uncertainty-guided Query Denoising, and Uncertainty-reduced Query Initialization to tackle the uncertainty problem from multiple aspects, leading to improved tracking performance.
- We demonstrate the effectiveness of our UA-Track framework quantitatively and qualitatively through extensive experiments on nuScenes benchmark and achieve leading performance with a remarkable 66.3% AMOTA on test split.

2 Related Work

3D Multi-Object Tracking. Multi-object tracking (MOT) in 3D scenes takes multi-view images from surrounding cameras or LiDAR point clouds to track multiple objects across frames [9, 22, 34, 40, 41, 44, 45, 52]. Taking advances in 3D object detection [16, 25–27, 29, 31, 32, 46], most 3D MOT methods follow the *tracking by detection* paradigm [4, 36, 52, 53, 56, 57], where tracking is treated as a post-processing step after object detection. Take the detected objects at each frame, traditional 3D MOT usually uses motion models, e.g., Kalman filter [49, 50], to predict the status of corresponding trajectory and associate the candidate detections using 3D IoU [36, 49] or L2 distance [53, 57]. To overcome the independent nature of the detection and tracking and to implicitly solve the association between frames, the recent *tracking with query* paradigm models the tracking process with transformer queries [6, 23, 35, 54, 55]. MUTR3D [55] extends the object detection method DETR3D [46] for tracking by utilizing a 3D track query to jointly model object features across timestamps and multi-view. PF-Track [35] extends the temporal horizon to provide a strong spatio-temporal object representation. STAR-TRACK [6] proposes a latent motion model to

account for the effects of ego and object motion on the latent appearance representation. DQTrack [23] separates object and trajectory representation using decoupled queries, allowing more accurate end-to-end 3D tracking. Although these methods achieved impressive performance, when applied to complex scenarios, especially the occlusions and the small target objects, the tracking performance becomes unsatisfactory. In this work, we argue that tackling the overlooked uncertainty issue can achieve improved tracking results. As a result, we propose an uncertainty-aware framework and consequently achieve leading performance.

Uncertainty Modeling. Uncertainty issue, which refers to neural networks that do not deliver certainty estimates or suffer from under-confidence, has been drawing increasing attention [2, 5, 11, 13, 38, 42, 47, 51]. To overcome this, many researchers have been working on understanding and quantifying uncertainty in their fields. Recently, different types and sources of uncertainty have been identified, and different approaches for measuring and quantifying uncertainty have been proposed. BayDNN [42] uses the uncertainty to help the fusion of visual modality and audio modality for audiovisual activity recognition. DUFR [5] incorporates uncertainty estimation to help reduce the adverse effects of noisy samples in face recognition. DUGM [47] proposes a data-uncertainty guided multi-phase learning method for semi-supervised object detection. UGTR [51] builds a probabilistic representational model to capture the uncertainty for camouflaged object detection. UGPT [13] uses epistemic uncertainty to guide both the training and inference of complex action recognition. However, the uncertainty in 3D MOT has not been explored yet. Moreover, due to the complex driving scenarios and the unique challenge of tracking tasks, previous solutions for specific domains cannot be directly applied here. In this work, we identify that the main uncertainty issue of 3D MOT lies in the occlusion situations and the small size of target objects, which usually leads to track losing of undetected or occluded objects. We further introduce an uncertainty-aware 3D MOT framework with three dedicated modules to cope with our specific uncertainty issue.

3 UA-Track

In this section, we introduce our proposed UA-Track in detail. We first give a brief problem definition and an overview of the framework in Sec. 3.1. Then, by considering the uncertainty issue, we clarify our key contributions in Sec. 3.2, Sec. 3.3, and Sec. 3.4.

3.1 Preliminaries

Under the *tracking with query* paradigm, an overview of proposed UA-Track is presented in Fig. 2, which is conceptually simple: encoder and transformer decoder are adopted to encode input images and decode 3D MOT outputs with queries. At each timestamp t , given c images from surrounding cameras, the tracking objective is to estimate a set of bounding boxes $\mathbf{b}_t^{id} \in \mathbf{B}_t$ with consistent *id* across frames.

Specifically, following previous studies [6, 35], our UA-Track utilizes a set of object queries to tackle multi-object tracking from multi-view images. Each

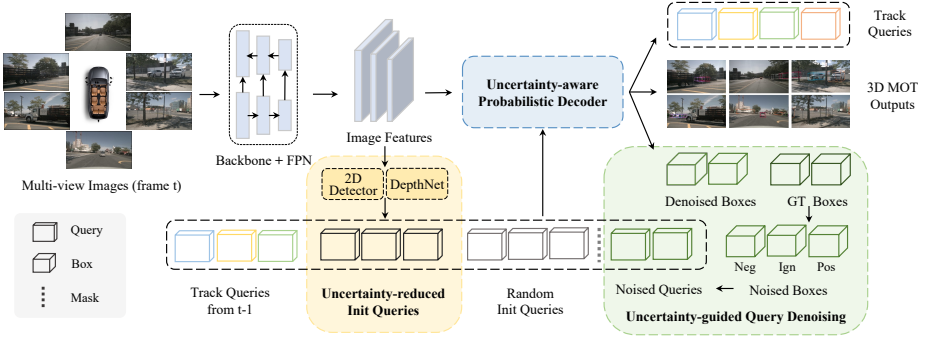


Fig. 2: UA-Track framework. The proposed Uncertainty-aware Probabilistic Decoder (UPD), Uncertainty-guided Query Denoising (UQD), and Uncertainty-reduced Query Initialization (UQI) are incorporated together to tackle the uncertainty issue. Neg: negative, Ign: ignore, Pos: positive, Mask: separate the normal queries and the denoising part to prevent information leakage.

query $\mathbf{q}_t^i \in \mathbf{Q}_t$ represents a unique 3D object with a feature vector \mathbf{f}_t^i and a 3D location \mathbf{c}_t^i , i.e., $\mathbf{q}_t^i = \{\mathbf{f}_t^i, \mathbf{c}_t^i\}$, and an object is tracked by updating its unique query. The object queries $\mathbf{Q}_t = \{\mathbf{q}_t^i\}$ are propagated from the previous frame $t - 1$ (colored squares) and numerous initial queries (gray squares in Fig. 2):

$$\mathbf{Q}_t \leftarrow \text{Prop}(\mathbf{Q}_{t-1}, \mathbf{Q}_{init}). \quad (1)$$

The queries from the previous frame represent tracked instances, while numerous initial queries aim to discover new objects.

Then, to predict 3D bounding boxes, decoder-only transformer architectures such as DETR3D [46] and PETR [31], are utilized to decode image features \mathbf{F}_t with object queries:

$$\mathbf{B}_t, \mathbf{Q}_t \leftarrow \text{Decoder}(\mathbf{F}_t, \mathbf{Q}_t), \quad (2)$$

where \mathbf{B}_t and \mathbf{Q}_t are the detected 3D bounding boxes and updated query features respectively.

As shown in Fig. 2, we propose three dedicated modules to tackle the uncertainty issue from multiple aspects. To model and capture the uncertainty in object prediction, we introduce an Uncertainty-aware Probabilistic Decoder (blue module). Moreover, we present an Uncertainty-guided Query Denoising strategy (green module) to enhance the model robustness and convergence against uncertainty of the training process. We also propose Uncertainty-reduced Query Initialization (yellow module) to improve the query initialization with reduced uncertainty. In the following sections, we give detailed elaboration.

3.2 Uncertainty-aware Probabilistic Decoder

In complex driving scenarios, the trajectories of multiple targets exhibit substantial variations in their temporal duration and sequence. These variations often lead to occlusions. Additionally, the target objects can vary in size, e.g.,

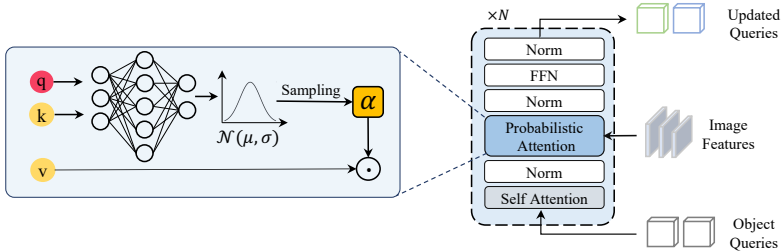


Fig. 3: Uncertainty-aware Probabilistic Decoder (UPD) architecture. The traditional cross-attention is upgraded with probabilistic attention to quantifying the uncertainty. The probabilistic attention utilizes a multi-layer perceptron that takes the query q and key k as input to generate the mean and standard deviation, which are used to form a Gaussian distribution. Subsequently, the attention value α is sampled from the constructed Gaussian distribution.

big trucks and small children. These diversities pose a challenge for deterministic attention mechanisms utilized in traditional transformers, as they struggle to capture the noise and variations present in the input data. Previous decoders employ conventional transformers, which compute determinate attention α between queries (Q) and keys (K) as $\alpha = \frac{Q \cdot K}{\sqrt{d}}$, where d is the dimension of queries and keys, which limits the ability to quantify uncertainty in predictions effectively.

To address this limitation, inspired by previous uncertainty quantify works [2, 13, 38], we introduce **Uncertainty-aware Probabilistic Decoder (UPD)** for 3D MOT with the probabilistic attention computation, which assume attention α follows a Gaussian distribution: $\alpha_{ij} \sim \mathcal{N}(\mu_{ij}, \sigma_{ij})$. Through the reparameterization trick [18]: $\alpha_{ij} = \mu_{ij} + \sigma_{ij}\epsilon$, $\epsilon \sim \mathcal{N}(0, 1)$. As illustrated in Fig. 3, a multi-layer perceptron is adopted to fit the mean and standard deviation with q_i, k_j as input: $\mu_{ij}, \sigma_{ij}^2 = MLP(q_i, k_j)$. Thus, we introduce the uncertainty-aware probabilistic parameters μ_{ij} and σ_{ij} into the decoder, allowing uncertainty adaptation in the training process. Practically, we employ scaled dot-product attention to constrain the probabilistic attention and utilize the negative log-likelihood loss to supervise the decoder as:

$$\mathcal{L}_{UPD} = \sum_{i,j} \log\left(\frac{1}{\sqrt{2\pi\sigma_{ij}^2}}\right) \exp\left(-\frac{(\alpha_{ij} - \frac{q_i k_j}{\sqrt{d}})^2}{2\sigma_{ij}^2}\right). \quad (3)$$

As a summary, our UPD module captures and models the uncertainty in object predictions by representing attention scores as Gaussian distributions, which are more robust and capable of handling variations and noise in the 3D MOT, and the Eq. (2) can be improved as:

$$\mathbf{B}_t, \mathbf{Q}_t \leftarrow \text{Decoder}_{UPD}(\mathbf{F}_t, \mathbf{Q}_t). \quad (4)$$

3.3 Uncertainty-guided Query Denoising

In complex scenarios of 3D MOT, various uncertainties such as occlusions and arbitrary sizes of tracked objects can significantly hinder the learning and rapid

convergence of query-based methods. Solely on the proposed UPD might not be sufficient to capture all the uncertainties about the precise instance features and localization of the tracked objects. To address this challenge, we draw inspiration from the previous work DN-DETR [21] and propose **Uncertainty-guided Query Denoising (UQD)** training strategy, which incorporates query denoising to enhance training process for stable optimization against uncertainty.

Specifically, we start by perturbing the ground truth boxes to generate noised queries. To distinguish different levels of uncertainty, we define lower and upper bound thresholds, denoted as β_{lower} and β_{upper} respectively. These thresholds help categorize the noised queries into three classes based on their uncertainty levels. We identified positive samples ("Pos" in Fig. 2), i.e., low-uncertainty samples, when the 3D Intersection over Union (IoU) between a noised query and its corresponding ground truth exceeds the β_{upper} threshold, i.e., $\text{IoU}_{\mathbf{q}_t^i} > \beta_{\text{upper}}$. Conversely, negative samples ("Neg" in Fig. 2), i.e., high-uncertainty samples, are defined when the 3D IoU falls below the β_{lower} threshold, i.e., $\text{IoU}_{\mathbf{q}_t^i} < \beta_{\text{lower}}$. Intermediate IoU values are disregarded ("Ign" in Fig. 2), as they do not provide clear indications of certainty or uncertainty, and can disrupt the normal query learning process as demonstrated in Tab. 5. The resulting set of noised queries that meet these requirements is denoted as $\mathbf{Q}_{\text{ug-noised}}$, and then the decoder process can be expanded as:

$$\mathbf{B}_t^U, \mathbf{Q}_t^U \leftarrow \text{Decoder}(\mathbf{F}_t, \mathbf{Q}_{\text{ug-noised}}). \quad (5)$$

For optimization, the loss for positive samples and negative samples are calculated to form the target:

$$\mathcal{L}_{UQD} = \mathcal{L}_{\text{box}}^{\text{pos}} + \mathcal{L}_{\text{cls}}^{\text{pos}} + \mathcal{L}_{\text{cls}}^{\text{neg}}, \quad (6)$$

where $\mathcal{L}_{\text{cls}}^{\text{pos}}$ and $\mathcal{L}_{\text{box}}^{\text{pos}}$ are respectively focal loss [28] and L1 loss for the classification and box loss of \mathbf{B}_t^U , while $\mathcal{L}_{\text{cls}}^{\text{neg}}$ is focal loss to distinguish the background.

Moreover, it's noted that we need to apply the attention mask as DN-DETR [21] to separate the matching part and the denoising part to prevent information leakage. Denote the attention mask by $A = a_{ij}, i \in [0 : M], j \in [0 : M]$, where M is the number of total queries. Let $[N : M]$ represent the denoising part, $a_{ij} = 1$ means the i -th query cannot see the j -th query and $a_{ij} = 0$ otherwise, then: $a_{ij} = \begin{cases} 1, & \text{if } i < N \text{ and } j \geq N; \\ 0, & \text{otherwise.} \end{cases}$

By incorporating the query denoising and handling the noised queries based on their uncertainty levels, our UQD module enhances the robustness and convergence of the training procedure, leading to more stable and accurate results.

3.4 Uncertainty-reduced Query Initialization

In *tracking with query* frameworks, high-quality initial queries are crucial for achieving rapid convergence and improving tracking precision, especially considering the uncertainties of occlusion situations and the small size of target objects,

which usually leads to some undetected or occluded objects losing track. To address this, we propose **Uncertainty-reduced Query Initialization (UQI)** module which enhances the initialization of queries using learned certain priors obtained from network training. Specifically, after utilizing the shared image backbone and the Feature Pyramid Network (FPN) layers to extract image features from each camera, we introduce additional auxiliary tasks, i.e., the 2D detection and the depth prediction, as follows:

$$\mathbf{B}_t^{2d}, \mathbf{D}_t \leftarrow \text{Networks}_{\text{auxiliary}}(\mathbf{F}_t), \quad (7)$$

where $\mathbf{B}_t^{2d}, \mathbf{D}_t$ denotes the 2D bounding boxes and the depth respectively. The 2D detection head follows YOLOX [12]. The depth network combines multiple residual blocks and is supervised with the projected LiDAR points. The optimization objectives of the two auxiliary tasks are:

$$\mathcal{L}_{UQI} = \mathcal{L}_{Det}^{2D} + \mathcal{L}_{Depth}. \quad (8)$$

Then, we estimate 3D location $\mathbf{C}_t = \{\mathbf{c}_t^i\}$ through the coordinate transformation: $\mathbf{C}_t = T_{cam}^{lidar} K^{-1} \mathbf{D}_t [u, v, 1]^T$, where T_{cam}^{lidar} and K^{-1} represent the transformation matrix from the camera coordinate system to the lidar coordinate system and the camera’s intrinsic parameters respectively, and (u, v) denotes the center location of the 2D boxes. Then we initialize our object queries with the preliminary 3D location, denoted as $\mathbf{Q}_{ur-init}$ (dark gray squares in Fig. 2). We also retain the random initialization \mathbf{Q}_{init} to explore missing objects. To summarize, the query initialization and propagation process in Eq. (1) can be improved as follows:

$$\mathbf{Q}_t \leftarrow \mathbf{Prop}(\mathbf{Q}_{t-1}, \mathbf{Q}_{ur-init}, \mathbf{Q}_{init}). \quad (9)$$

The UQI module utilizes learned certain priors, i.e., 2D object location and depth information, to enhance the initialization of queries.

3.5 Overall Optimization

To summarize, the overall optimization target of our UA-Track is formulated as:

$$\mathcal{L} = \lambda_{tracking} \mathcal{L}_{tracking} + \lambda_{UPD} \mathcal{L}_{UPD} + \lambda_{UQD} \mathcal{L}_{UQD} + \lambda_{UQI} \mathcal{L}_{UQI}, \quad (10)$$

where $\mathcal{L}_{tracking} = \mathcal{L}_{cls} + \mathcal{L}_{box}$, \mathcal{L}_{cls} and \mathcal{L}_{box} are classification loss and box loss for the tracked objects, \mathcal{L}_{UPD} , \mathcal{L}_{UQD} and \mathcal{L}_{UQI} are defined in Eq. (3), Eq. (6) and Eq. (8), and λ indicate the weight balance coefficients.

4 Experiment

In this section, we first introduce the experimental setup in Sec. 4.1. Then, we compare UA-Track with leading approaches in Sec. 4.2. The analyses of uncertainty and each component are presented in Sec. 4.3 and Sec. 4.4. In the end, we provide qualitative results in Sec. 4.5.

Table 1: Comparisons with previous methods on the nuScenes *val* set. Our UA-Track outperforms all existing camera-based 3D MOT methods in all metrics.

Method	Backbone	AMOTA \uparrow	AMOTP \downarrow	RECALL \uparrow	MOTA \uparrow	MOTP \downarrow	IDS \downarrow
DEFT [4]	DLA-34	0.201	–	–	0.171	–	–
QD-3DT [14]	DLA-34	0.242	1.518	39.9%	0.218	–	5646
TripletTrack [34]	R18	0.285	1.485	–	–	–	–
CC-3DT [9]	R101	0.429	1.257	53.4%	0.385	–	2219
QTrack [52]	V2-99	0.511	1.090	58.5%	0.465	–	1144
<i>Tracking with Query</i>							
MUTR3D [55]	R101	0.294	1.498	42.7%	0.267	0.709	3822
STAR-TRACK [6]	R101	0.379	1.358	50.1%	0.360	–	372
DQTrack [23]	V2-99	0.446	1.251	62.2%	–	–	1193
PF-Track-S [35]	V2-99	0.408	1.343	50.7%	0.376	–	166
PF-Track-F [35]	V2-99	0.479	1.227	59.0%	0.435	–	181
Sparse4D-v3 [29]	R101	0.567	1.027	65.8%	0.515	0.621	557
UA-Track-S (Ours)	V2-99	0.458	1.230	56.6%	0.433	0.664	172
UA-Track-S (Ours)	ViT-L	0.600	1.020	68.8%	0.538	0.614	167
UA-Track-F (Ours)	ViT-L	0.652	0.924	72.2%	0.574	0.577	134

"S" and "F" represent the settings of small-resolution and full-resolution respectively.

4.1 Experimental Setup

Dataset. We conduct experiments on the popular nuScenes benchmark [3], which is a large-scale autonomous-driving dataset for 3D detection and tracking, consisting of 700, 150, and 150 scenes for training, validation, and testing, respectively. Each frame contains one point cloud and six calibrated images from the surrounding cameras with a full 360-degree field of view. It provides 3D tracking bounding boxes from 7 categories for the tracking task.

Metrics. We follow the official evaluation metrics from nuScenes. For the 3D tracking task, we report Average Multi-object Tracking Accuracy (AMOTA) [48], Average Multi-object Tracking Precision (AMOTP), and the modified CLEAR MOT metrics [1], e.g., MOTA, MOTP, and IDS. For a detailed understanding, please refer to [1, 3].

Implementation Details. In this paper, we assess the generalization capability of our UA-Track through experiments using different encoders, e.g., V2-99 [20] and ViT [7], and different decoders e.g., PETR [30] and DETR3D [46]. All experiments are conducted on 8 NVIDIA A100-80GB GPUs. For each training sample, it contains three consecutive adjacent frames each with contains six surrounding images, and we use a fixed number of 500 initial queries for each sample. We adopt the AdamW optimizer [33] for network training, with the initial learning rate setting of 0.01 and the cosine weight decay set to 0.001. By default, the thresholds β_{lower} and β_{upper} are set to 0.3 and 0.7, and the weight coefficients λ that are all set to 1.0, respectively.

Table 2: Comparisons with state-of-the-art camera-based methods on the nuScenes *test* set. Our UA-Track surpasses the previous best solution by a significant margin of 8.9% AMOTA.

Method	Backbone	AMOTA↑	AMOTP↓	RECALL↑	MOTA↑	MOTP ↓	IDS↓
CenterTrack [57]	DLA-34	0.046	1.543	23.3%	0.043	0.753	3807
PermaTrack [43]	DLA-34	0.066	1.491	18.9%	0.060	0.724	3598
DEFT [4]	DLA-34	0.177	1.564	33.8%	0.156	0.770	6901
QD-3DT [14]	DLA-34	0.217	1.550	37.5%	0.198	0.773	6856
TripletTrack [34]	R18	0.268	1.504	40.0%	0.245	0.800	1044
CC-3DT [9]	R101	0.410	1.274	53.8%	0.357	0.676	3334
QTrack [52]	V2-99	0.480	1.100	58.3%	0.431	0.597	1484
<i>Tracking with Query</i>							
MUTR3D [55]	R101	0.270	1.494	41.1%	0.245	0.709	6018
PF-Track-F [35]	V2-99	0.434	1.252	53.8%	0.378	0.674	249
STAR-TRACK [6]	V2-99	0.439	1.256	56.2%	0.406	0.664	607
DQTrack [23]	V2-99	0.523	1.096	62.2%	0.444	0.649	1204
Sparse4D-v3 [29]	V2-99	0.574	0.970	66.9%	0.521	0.525	669
UA-Track-F (Ours)	V2-99	0.608	0.925	75.8%	0.547	0.559	963
UA-Track-F (Ours)	ViT-L	0.663	0.815	72.3%	0.554	0.530	844

"F" represent on the full-resolution settings.

Due to the limited computation resources, we follow PF-Track [35] to apply two resolution settings, full-resolution and small-resolution. For full-resolution (“-F”), we crop the origin 1600×900 image to 1600×640 . For small-resolution (“-S”), we scale down the cropped image to 800×320 in a further step. We pre-train the image backbone with single-frame detection task for 12 epochs (small-resolution setting) and 24 epochs (full-resolution setting) respectively, and further train the end-to-end tracker with consecutive frames (set to be 3 frames) for another 12 epochs (small-resolution) and 24 epochs (full-resolution). All the ablation studies are conducted on the small-resolution setting with V2-99 backbone.

4.2 State-of-the-art Comparison

Tracking on nuScenes val set. In Tab. 1, we compare our UA-Track with state-of-the-art methods on nuScenes val set. First, our method significantly outperforms existing algorithms across all tracking metrics, whether they are end-to-end or non-end-to-end methods. Specifically, UA-Track achieves impressive performance with 65.2% AMOTA and 0.924 AMOTP. When compared with the previous query-based tracker Sparse4D-v3, the performance gap is further enlarged to 8.5% AMOTA. Second, we validate the generality of UA-Track by applying different encoder backbones, i.e., V2-99 and ViT. Equipped with V2-99, the proposed framework achieves consistent gains with 6.4% AMOTA (UA-Track-S vs PF-Track-S).

Tracking on nuScenes test set. In Tab. 2, we compare our UA-Track with state-of-the-art camera-based methods on nuScenes test set. Our proposed UA-

Table 3: Uncertainty quantification results and ablations on the proposed modules of UA-Track. s and σ donate entropy and standard deviation, respectively.

Method			Tracking					Uncertainty		
UPD	UQI	UQD	AMOTA \uparrow	AMOTP \downarrow	RECALL \uparrow	MOTA \uparrow	MOTP \downarrow	IDS \downarrow	$s\downarrow$	$\sigma\downarrow$
<i>MC Dropout [10]</i>										
\times	\times	\times	0.394	1.363	51.4%	0.372	0.753	178	1.99	0.108
\checkmark	\times	\times	0.438	1.261	55.9%	0.419	0.681	175	1.86	0.085
\times	\checkmark	\times	0.418	1.251	54.6%	0.394	0.667	177	1.91	0.097
\times	\times	\checkmark	0.423	1.264	55.6%	0.397	0.671	183	1.88	0.093
\checkmark	\checkmark	\checkmark	0.458	1.230	56.6%	0.433	0.664	172	1.81	0.078
<i>Ensemble [19]</i>										
PF-Track-S [35]			0.408	1.343	50.7%	0.376	–	166	1.96	0.100
UA-Track-S			0.458	1.230	56.6%	0.433	0.664	172	1.75	0.072

Track maintains an end-to-end tracking pipeline without heuristic post-processing and achieves leading performance with 66.3% AMOTA, surpassing the previous best solution Sparse4D-v3 by a significant margin of 8.9% AMOTA.

4.3 Uncertainty Analysis

Analysis of the proposed modules of UA-Track. In Tab. 3, we validate our proposed modules for our model’s performance on nuScenes val set. It is clear that incorporating each uncertainty-aware module facilitates the tackling of the uncertainty issue and leads to performance gain in tracking. Specifically, the Uncertainty-aware Probabilistic Decoder (UPD) module significantly improves the baseline with 4.4% AMOTA, and the Uncertainty-reduced Query Initialization (UQI) and Uncertainty-guided Query Denoising (UQD) modules obtained consist boost with 2.4% and 2.9% AMOTA respectively. Moreover, combining the three modules leads to further improvements, indicating that they effectively alleviate the uncertainty issue from many aspects.

Uncertainty quantification. Quantifying uncertainty can be challenging for transformer-based models which do not inherently provide uncertainty estimates like Bayesian methods. It’s an independent research domain [39]. Thus, we can only employ computationally intensive strategies to approximate uncertainty, such as the Monte Carlo Dropout (MC dropout) [10] and Ensemble strategy [19]. As shown in Tab. 3, our method, along with the proposed three modules, effectively reduces the uncertainty. Furthermore, it can be observed that the tracking metric aligns well with the results of uncertainty quantification. Therefore, due to computational constraints, we focus on the corresponding indicators of our tracking task in other parts of this paper.

The occlusions. In Fig. 4 (a), we systematically analyze the performance of UA-Track under different occlusion conditions, i.e., different visibilities. Tracking

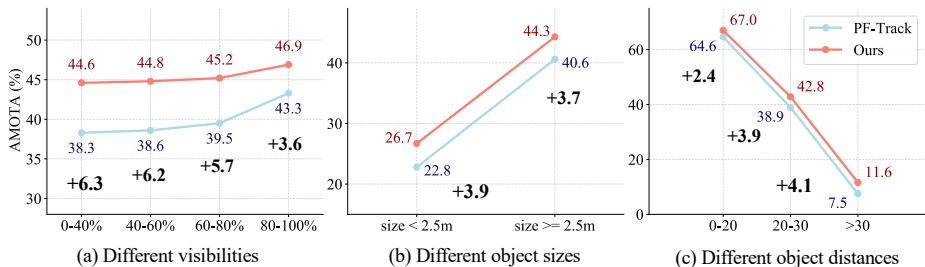


Fig. 4: The uncertainty analysis. UA-Track consistently outperforms state-of-the-art tracker PF-Track [35] under different uncertainty situations, especially under severe occlusions and small object size settings.

Table 4: Ablations on different decoders.

Decoder	AMOTA↑	AMOTP↓	RECALL↑	MOTA↑	MOTP ↓	IDS↓
PETR [30]	0.452	1.246	57.1%	0.429	0.682	196
DETR3D [46]	0.458	1.230	56.6%	0.433	0.664	172

objects in occlusion scenarios is challenging for previous trackers that do not incorporate uncertainty modeling. Thanks to our uncertainty-aware framework, UA-Track consistently improves PF-Track [35]. Lower visibilities indicate more severe occlusions, which are more challenging for tracking models. Notably, our UA-Track achieves a significant performance boost of 6.3% AMOTA, which is even larger than the improvement in the high visibility scenario. This result highlights the importance of uncertainty modeling in 3D MOT.

The small size of tracked objects. In Fig. 4 (b) and (c), we also analyze the performance under different object sizes and distances. Our UA-Track achieves consistent improvements over PF-Track [35] for both small and large objects. Furthermore, UA-Track brings larger improvements in more challenging situations characterized by severe uncertainty issues, such as smaller objects (Fig. 4 (b), + 3.9% AMOTA) and more distant objects (Fig. 4 (c), + 4.1% AMOTA), both of which demonstrate the effectiveness of our uncertainty-aware framework in addressing diverse challenges in 3D MOT.

4.4 Ablation Study

Ablations on different decoders. In Tab. 4, we validate the generality of UA-Track by applying different decoders. Specifically, we employ two popular decoders: PETR [30] and DETR3D [46], which are widely adopted by query-based tracking methods. Our approach achieves excellent results with both decoders, yielding comparable performance. The results obtained with DETR3D are slightly higher, leading us to select DETR3D as our default decoder.

Ablations on uncertainty thresholds of UQD module. In Tab. 5, we validate various settings of the uncertainty threshold of UQD module. (1) In the

Table 5: Ablations on uncertainty thresholds of UQD module. (1) Without thresholds, (2) without selecting by uncertainty levels, (3) Our UQD.

Threshold	AMOTA \uparrow	AMOTP \downarrow	RECALL \uparrow	MOTA \uparrow	IDS \downarrow
(1)	0.440	1.249	55.9%	0.419	181
(2)	0.445	1.239	56.5%	0.425	174
(3)	0.458	1.230	56.6%	0.433	172
<i>Lower Bound Thresholds</i>					
0.20	0.450	1.236	56.3%	0.429	179
0.30	0.458	1.230	56.6%	0.433	172
0.40	0.448	1.241	56.4%	0.427	173
<i>Upper Bound Thresholds</i>					
0.60	0.436	1.261	56.1%	0.419	204
0.65	0.455	1.243	57.5%	0.434	198
0.70	0.458	1.230	56.6%	0.433	172
0.75	0.444	1.253	55.9%	0.416	214

Table 6: Ablations on network strides of UQI module.

Stride	AMOTA \uparrow	AMOTP \downarrow	RECALL \uparrow	MOTA \uparrow	IDS \downarrow
8	0.456	1.245	56.1%	0.422	178
16	0.458	1.230	56.6%	0.433	172
32	0.446	1.268	56.2%	0.419	214

first setting, we do not consider the uncertainty thresholds, meaning that all noised queries undergo box optimization. (2) In the second setting, we do not selectively denoise queries based on their uncertainty levels; instead, a single threshold is used to classify all noised queries into positive and negative samples for optimization. (3) In our UQD module, we selectively denoise queries based on their uncertainty levels. The improved performance demonstrates our UQD, which optimizes samples based on different uncertainty levels, effectively addresses the uncertainty issue, and achieves superior results. We also investigate varying lower and upper bound thresholds, i.e., β_{lower} and β_{upper} . The model achieves the best result when β_{lower} is set to 0.30 and β_{upper} is set to 0.70.

Ablations on network strides of UQI module. In Tab. 6, we conduct an ablation study to analyze the effects of the network stride of UQI module. As described in Eq. (7), our UQI module incorporates two additional auxiliary tasks based on the extracted feature \mathbf{F}_t . To reduce computational overhead, we can directly reuse features from different layers with varying strides in the Feature Pyramid Network (FPN), thereby alleviating the burden on the auxiliary task heads. We present the performance achieved with different strides for the image features. The experimental results reveal that the model performs optimally when using a stride of 16.

4.5 Qualitative Comparison

In Fig. 5, we provide the qualitative results on nuScenes dataset. We compare our UA-Track with the previous state-of-the-art end-to-end tracker, PF-Track [35]. In Fig. 5 (a), the tracking results across consecutive frames first reveal that PF-Track struggles to track the small object as evidenced by the tracking failure at time t_i . PF-Track exhibits commendable tracking accuracy when the line of sight is clear at time t_{i+3} . However, as the occlusion gradually intensifies, the accumulated error arising from uncertainty significantly escalates (t_{i+6} and t_{i+12}). Especially at t_{i+12} , the predicted bounding boxes for two pedestrians completely overlap. In contrast, our UA-Track consistently maintains a high level of tracking precision throughout the entire duration of continuous tracking. In complex scenarios of Fig. 5 (b), which are characterized by multiple uncertainty factors such as occlusions in crowded and spacious environments, as well as the small size of vehicles and pedestrians, UA-Track achieves more precise tracking bounding boxes and successfully recognizes more tracked objects compared to PF-Track [35]. Furthermore, the visualization of our attention scores demonstrates a higher concentration on the object center, indicating that our model pays more attention to the target objects. In contrast, PF-Track [35] exhibits low attention scores for challenging samples, failing to capture and track objects. The outstanding 3D MOT results of UA-Track demonstrate the effectiveness of our uncertainty-aware framework, which addresses the challenges posed by uncertainty across various complex tracking scenarios.

5 Conclusion

In this paper, we propose an uncertainty-aware 3D MOT framework, UA-Track, that effectively addresses the uncertainty problem in multiple aspects. First, the Uncertainty-aware Probabilistic Decoder models uncertainty using probabilistic attention, providing a comprehensive understanding of predictive uncertainty. Then, the Uncertainty-guided Query Denoising strategy enhances training robustness and convergence against uncertainty. The Uncertainty-reduced Query Initialization module improves object localization accuracy by incorporating predicted 2D location and depth cues. Experimental results on nuScenes benchmark demonstrate that UA-Track achieves state-of-the-art performance, i.e., 66.3% AMOTA on the test split, with a significant improvement of 8.9% AMOTA.

Social Impact and Limitations. Our framework highlights the importance of addressing uncertainty, especially the occlusions and small size of target objects in 3D MOT, and showcases its potential for advancing autonomous driving perception. Although our method effectively models uncertainty in three aspects, we encourage future research to develop more powerful frameworks that can further quantify and address more uncertainty issues. We hope that our work can shed light on the uncertainty issue and inspire future research.

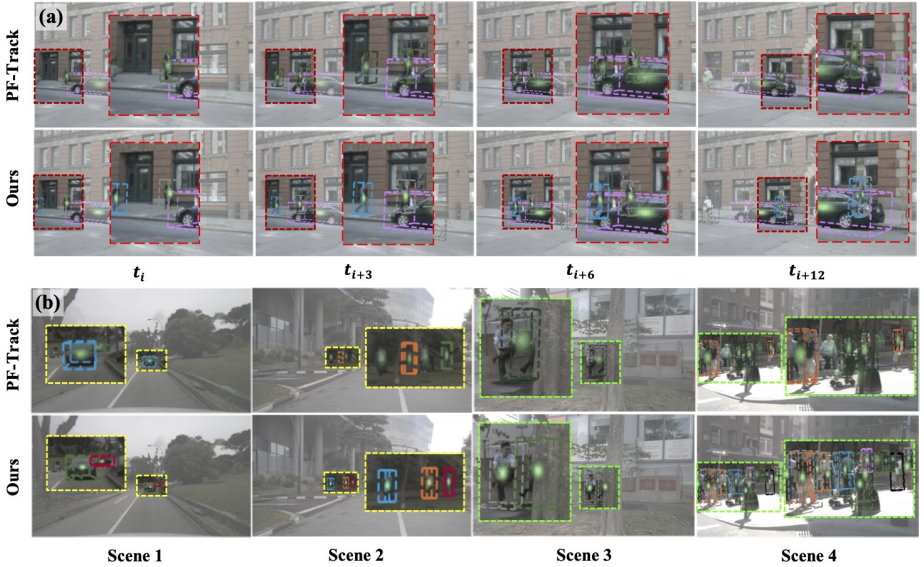


Fig. 5: Qualitative results on the nuScenes dataset. (a) The tracking results for an occlusion scenario of two pedestrians of consecutive frames ($t_i - t_{i+12}$), which are often encountered in real life. (b) The tracking results on several challenging tracking scenes with uncertainty, including the small size of vehicles and pedestrians (scene 1 and scene 2) and occlusions in spacious and crowded environments (scene 3 and scene 4). Moreover, we plot the attention scores of object queries, which indicate how strongly the model focuses on the target objects. A higher concentration of color represents a higher attention score and a stronger confidence in the corresponding object.

References

1. Bernardin, K., Stiefelhagen, R.: Evaluating multiple object tracking performance: the clear mot metrics. *EURASIP Journal on Image and Video Processing* **2008**, 1–10 (2008) [9](#)
2. Blundell, C., Cornebise, J., Kavukcuoglu, K., Wierstra, D.: Weight uncertainty in neural network. In: *International conference on machine learning*. pp. 1613–1622. PMLR (2015) [4](#), [6](#)
3. Caesar, H., Bankiti, V., Lang, A.H., Vora, S., Liong, V.E., Xu, Q., Krishnan, A., Pan, Y., Baldan, G., Beijbom, O.: nuscenes: A multimodal dataset for autonomous driving. In: *Proceedings of the IEEE/CVF conference on computer vision and pattern recognition*. pp. 11621–11631 (2020) [9](#), [20](#)
4. Chaabane, M., Zhang, P., Beveridge, J.R., O’Hara, S.: Deft: Detection embeddings for tracking. *arXiv preprint arXiv:2102.02267* (2021) [2](#), [3](#), [9](#), [10](#)
5. Chang, J., Lan, Z., Cheng, C., Wei, Y.: Data uncertainty learning in face recognition. In: *Proceedings of the IEEE/CVF conference on computer vision and pattern recognition*. pp. 5710–5719 (2020) [4](#)
6. Doll, S., Hanselmann, N., Schneider, L., Schulz, R., Enzweiler, M., Lensch, H.P.: Star-track: Latent motion models for end-to-end 3d object tracking with adaptive spatio-temporal appearance representations. *IEEE Robotics and Automation Letters* (2023) [2](#), [3](#), [4](#), [9](#), [10](#)
7. Dosovitskiy, A., Beyer, L., Kolesnikov, A., Weissenborn, D., Zhai, X., Unterthiner, T., Dehghani, M., Minderer, M., Heigold, G., Gelly, S., et al.: An image is worth 16x16 words: Transformers for image recognition at scale. *arXiv preprint arXiv:2010.11929* (2020) [9](#)
8. Feng, C., Jie, Z., Zhong, Y., Chu, X., Ma, L.: Aedet: Azimuth-invariant multi-view 3d object detection. In: *Proceedings of the IEEE/CVF Conference on Computer Vision and Pattern Recognition*. pp. 21580–21588 (2023) [21](#), [22](#)
9. Fischer, T., Yang, Y.H., Kumar, S., Sun, M., Yu, F.: Cc-3dt: Panoramic 3d object tracking via cross-camera fusion. In: *6th Annual Conference on Robot Learning* (2022) [3](#), [9](#), [10](#)
10. Gal, Y., Ghahramani, Z.: Dropout as a bayesian approximation: Representing model uncertainty in deep learning. In: *international conference on machine learning*. pp. 1050–1059. PMLR (2016) [11](#)
11. Gawlikowski, J., Tassi, C.R.N., Ali, M., Lee, J., Humt, M., Feng, J., Kruspe, A., Triebel, R., Jung, P., Roscher, R., et al.: A survey of uncertainty in deep neural networks. *arXiv preprint arXiv:2107.03342* (2021) [2](#), [4](#)
12. Ge, Z., Liu, S., Wang, F., Li, Z., Sun, J.: Yolox: Exceeding yolo series in 2021. *arXiv preprint arXiv:2107.08430* (2021) [8](#)
13. Guo, H., Wang, H., Ji, Q.: Uncertainty-guided probabilistic transformer for complex action recognition. In: *Proceedings of the IEEE/CVF Conference on Computer Vision and Pattern Recognition*. pp. 20052–20061 (2022) [2](#), [4](#), [6](#)
14. Hu, H.N., Yang, Y.H., Fischer, T., Darrell, T., Yu, F., Sun, M.: Monocular quasi-dense 3d object tracking. *IEEE Transactions on Pattern Analysis and Machine Intelligence* **45**(2), 1992–2008 (2022) [9](#), [10](#)
15. Huang, J., Huang, G.: Bevdet4d: Exploit temporal cues in multi-camera 3d object detection. *arXiv preprint arXiv:2203.17054* (2022) [21](#), [22](#)
16. Huang, J., Huang, G., Zhu, Z., Ye, Y., Du, D.: Bevdet: High-performance multi-camera 3d object detection in bird-eye-view. *arXiv preprint arXiv:2112.11790* (2021) [3](#)

17. Jiang, X., Li, S., Liu, Y., Wang, S., Jia, F., Wang, T., Han, L., Zhang, X.: Far3d: Expanding the horizon for surround-view 3d object detection. arXiv preprint arXiv:2308.09616 (2023) [21](#), [22](#)
18. Kingma, D.P., Salimans, T., Welling, M.: Variational dropout and the local reparameterization trick. *Advances in neural information processing systems* **28** (2015) [6](#)
19. Lakshminarayanan, B., Pritzel, A., Blundell, C.: Simple and scalable predictive uncertainty estimation using deep ensembles. *Advances in neural information processing systems* **30** (2017) [11](#)
20. Lee, Y., Hwang, J.w., Lee, S., Bae, Y., Park, J.: An energy and gpu-computation efficient backbone network for real-time object detection. In: *Proceedings of the IEEE/CVF conference on computer vision and pattern recognition workshops*. pp. 0–0 (2019) [9](#)
21. Li, F., Zhang, H., Liu, S., Guo, J., Ni, L.M., Zhang, L.: Dn-detr: Accelerate detr training by introducing query denoising. In: *Proceedings of the IEEE/CVF Conference on Computer Vision and Pattern Recognition*. pp. 13619–13627 (2022) [7](#)
22. Li, X., Xie, T., Liu, D., Gao, J., Dai, K., Jiang, Z., Zhao, L., Wang, K.: Polymot: A polyhedral framework for 3d multi-object tracking. In: *2023 IEEE/RSJ International Conference on Intelligent Robots and Systems (IROS)*. pp. 9391–9398. IEEE (2023) [2](#), [3](#)
23. Li, Y., Yu, Z., Phillion, J., Anandkumar, A., Fidler, S., Jia, J., Alvarez, J.: End-to-end 3d tracking with decoupled queries. In: *Proceedings of the IEEE/CVF International Conference on Computer Vision*. pp. 18302–18311 (2023) [2](#), [3](#), [4](#), [9](#), [10](#), [21](#), [22](#)
24. Li, Y., Bao, H., Ge, Z., Yang, J., Sun, J., Li, Z.: Bevstereo: Enhancing depth estimation in multi-view 3d object detection with temporal stereo. In: *Proceedings of the AAAI Conference on Artificial Intelligence*. vol. 37, pp. 1486–1494 (2023) [21](#)
25. Li, Y., Ge, Z., Yu, G., Yang, J., Wang, Z., Shi, Y., Sun, J., Li, Z.: Bevdepth: Acquisition of reliable depth for multi-view 3d object detection. In: *Proceedings of the AAAI Conference on Artificial Intelligence*. vol. 37, pp. 1477–1485 (2023) [3](#), [21](#), [22](#)
26. Li, Z., Wang, W., Li, H., Xie, E., Sima, C., Lu, T., Qiao, Y., Dai, J.: Bevformer: Learning bird’s-eye-view representation from multi-camera images via spatiotemporal transformers. In: *European conference on computer vision*. pp. 1–18. Springer (2022) [3](#)
27. Liang, T., Xie, H., Yu, K., Xia, Z., Lin, Z., Wang, Y., Tang, T., Wang, B., Tang, Z.: Bevfusion: A simple and robust lidar-camera fusion framework. *Advances in Neural Information Processing Systems* **35**, 10421–10434 (2022) [3](#)
28. Lin, T.Y., Goyal, P., Girshick, R., He, K., Dollár, P.: Focal loss for dense object detection. In: *Proceedings of the IEEE international conference on computer vision*. pp. 2980–2988 (2017) [7](#)
29. Lin, X., Pei, Z., Lin, T., Huang, L., Su, Z.: Sparse4d v3: Advancing end-to-end 3d detection and tracking. arXiv preprint arXiv:2311.11722 (2023) [3](#), [9](#), [10](#), [21](#), [22](#)
30. Liu, Y., Wang, T., Zhang, X., Sun, J.: Petr: Position embedding transformation for multi-view 3d object detection. In: *European Conference on Computer Vision*. pp. 531–548. Springer (2022) [9](#), [12](#)
31. Liu, Y., Yan, J., Jia, F., Li, S., Gao, A., Wang, T., Zhang, X.: Petr2: A unified framework for 3d perception from multi-camera images. In: *Proceedings of the IEEE/CVF International Conference on Computer Vision*. pp. 3262–3272 (2023) [3](#), [5](#), [21](#), [22](#)

32. Liu, Z., Tang, H., Amini, A., Yang, X., Mao, H., Rus, D.L., Han, S.: Bevfusion: Multi-task multi-sensor fusion with unified bird’s-eye view representation. In: 2023 IEEE international conference on robotics and automation (ICRA). pp. 2774–2781. IEEE (2023) [3](#)
33. Loshchilov, I., Hutter, F.: Decoupled weight decay regularization. arXiv preprint arXiv:1711.05101 (2017) [9](#)
34. Marinello, N., Proesmans, M., Van Gool, L.: Triplettrack: 3d object tracking using triplet embeddings and lstm. In: Proceedings of the IEEE/CVF Conference on Computer Vision and Pattern Recognition. pp. 4500–4510 (2022) [3](#), [9](#), [10](#)
35. Pang, Z., Li, J., Tokmakov, P., Chen, D., Zagoruyko, S., Wang, Y.X.: Standing between past and future: Spatio-temporal modeling for multi-camera 3d multi-object tracking. In: Proceedings of the IEEE/CVF Conference on Computer Vision and Pattern Recognition. pp. 17928–17938 (2023) [1](#), [2](#), [3](#), [4](#), [9](#), [10](#), [11](#), [12](#), [14](#), [21](#), [22](#)
36. Pang, Z., Li, Z., Wang, N.: Simpletrack: Understanding and rethinking 3d multi-object tracking. In: European Conference on Computer Vision. pp. 680–696. Springer (2022) [2](#), [3](#)
37. Park, J., Xu, C., Yang, S., Keutzer, K., Kitani, K., Tomizuka, M., Zhan, W.: Time will tell: New outlooks and a baseline for temporal multi-view 3d object detection. arXiv preprint arXiv:2210.02443 (2022) [21](#), [22](#)
38. Pei, J., Wang, C., Szarvas, G.: Transformer uncertainty estimation with hierarchical stochastic attention. In: Proceedings of the AAAI Conference on Artificial Intelligence. vol. 36, pp. 11147–11155 (2022) [4](#), [6](#)
39. Pei, J., Wang, C., Szarvas, G.: Transformer uncertainty estimation with hierarchical stochastic attention. In: Proceedings of the AAAI Conference on Artificial Intelligence. vol. 36, pp. 11147–11155 (2022) [11](#)
40. Qing, L., Wang, T., Lin, D., Pang, J.: Dort: Modeling dynamic objects in recurrent for multi-camera 3d object detection and tracking. In: Conference on Robot Learning. pp. 3749–3765. PMLR (2023) [2](#), [3](#)
41. Sadjadpour, T., Li, J., Ambrus, R., Bohg, J.: Shasta: Modeling shape and spatio-temporal affinities for 3d multi-object tracking. IEEE Robotics and Automation Letters (2023) [3](#)
42. Subedar, M., Krishnan, R., Meyer, P.L., Tickoo, O., Huang, J.: Uncertainty-aware audiovisual activity recognition using deep bayesian variational inference. In: Proceedings of the IEEE/CVF international conference on computer vision. pp. 6301–6310 (2019) [2](#), [4](#)
43. Tokmakov, P., Li, J., Burgard, W., Gaidon, A.: Learning to track with object permanence. In: Proceedings of the IEEE/CVF International Conference on Computer Vision. pp. 10860–10869 (2021) [10](#)
44. Wang, L., Zhang, X., Qin, W., Li, X., Gao, J., Yang, L., Li, Z., Li, J., Zhu, L., Wang, H., et al.: Camo-mot: Combined appearance-motion optimization for 3d multi-object tracking with camera-lidar fusion. IEEE Transactions on Intelligent Transportation Systems (2023) [2](#), [3](#)
45. Wang, S., Liu, Y., Wang, T., Li, Y., Zhang, X.: Exploring object-centric temporal modeling for efficient multi-view 3d object detection. In: Proceedings of the IEEE/CVF International Conference on Computer Vision (ICCV). pp. 3621–3631 (October 2023) [3](#), [21](#), [22](#)
46. Wang, Y., Guizilini, V.C., Zhang, T., Wang, Y., Zhao, H., Solomon, J.: Detr3d: 3d object detection from multi-view images via 3d-to-2d queries. In: Conference on Robot Learning. pp. 180–191. PMLR (2022) [3](#), [5](#), [9](#), [12](#)

47. Wang, Z., Li, Y., Guo, Y., Fang, L., Wang, S.: Data-uncertainty guided multi-phase learning for semi-supervised object detection. In: Proceedings of the IEEE/CVF Conference on Computer Vision and Pattern Recognition. pp. 4568–4577 (2021) [2](#), [4](#)
48. Weng, X., Kitani, K.: A baseline for 3d multi-object tracking. arXiv preprint arXiv:1907.03961 **1**(2), 6 (2019) [9](#)
49. Weng, X., Wang, J., Held, D., Kitani, K.: 3d multi-object tracking: A baseline and new evaluation metrics. In: 2020 IEEE/RSJ International Conference on Intelligent Robots and Systems (IROS). pp. 10359–10366. IEEE (2020) [2](#), [3](#)
50. Wojke, N., Bewley, A., Paulus, D.: Simple online and realtime tracking with a deep association metric. In: 2017 IEEE international conference on image processing (ICIP). pp. 3645–3649. IEEE (2017) [2](#), [3](#)
51. Yang, F., Zhai, Q., Li, X., Huang, R., Luo, A., Cheng, H., Fan, D.P.: Uncertainty-guided transformer reasoning for camouflaged object detection. In: Proceedings of the IEEE/CVF International Conference on Computer Vision. pp. 4146–4155 (2021) [2](#), [4](#)
52. Yang, J., Yu, E., Li, Z., Li, X., Tao, W.: Quality matters: Embracing quality clues for robust 3d multi-object tracking. arXiv preprint arXiv:2208.10976 (2022) [2](#), [3](#), [9](#), [10](#)
53. Yin, T., Zhou, X., Krahenbuhl, P.: Center-based 3d object detection and tracking. In: Proceedings of the IEEE/CVF conference on computer vision and pattern recognition. pp. 11784–11793 (2021) [2](#), [3](#)
54. Zeng, F., Dong, B., Zhang, Y., Wang, T., Zhang, X., Wei, Y.: Motr: End-to-end multiple-object tracking with transformer. In: European Conference on Computer Vision. pp. 659–675. Springer (2022) [2](#), [3](#)
55. Zhang, T., Chen, X., Wang, Y., Wang, Y., Zhao, H.: Mutr3d: A multi-camera tracking framework via 3d-to-2d queries. In: Proceedings of the IEEE/CVF Conference on Computer Vision and Pattern Recognition. pp. 4537–4546 (2022) [2](#), [3](#), [9](#), [10](#), [21](#), [22](#)
56. Zhang, Y., Sun, P., Jiang, Y., Yu, D., Weng, F., Yuan, Z., Luo, P., Liu, W., Wang, X.: Bytetrack: Multi-object tracking by associating every detection box. In: European Conference on Computer Vision. pp. 1–21. Springer (2022) [3](#)
57. Zhou, X., Koltun, V., Krähenbühl, P.: Tracking objects as points. In: European conference on computer vision. pp. 474–490. Springer (2020) [2](#), [3](#), [10](#)
58. Zong, Z., Jiang, D., Song, G., Xue, Z., Su, J., Li, H., Liu, Y.: Temporal enhanced training of multi-view 3d object detector via historical object prediction. arXiv preprint arXiv:2304.00967 (2023) [21](#), [22](#)

6 Additional Details

6.1 Depthnet Details

The depth network of the proposed UQI module is composed of multiple residual blocks, and we provide an illustration in Fig. 6.

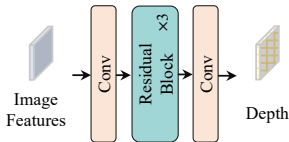


Fig. 6: Details of the depth network in UQI.

6.2 Uncertainty Analysis Details

The analysis studies in Fig. 4 are conducted on the small-resolution setting with V2-99 backbone. The experiments are performed on the nuScenes val set, in which we focus on specific uncertainty conditions to select clips for evaluation. We utilize the attributes of the bounding boxes provided by the nuScenes dataset, e.g., the visibility labels, and then calculate the average for each clip, finally group the results according to different ranges of the attributes. The uncertainty categorization process involved the following criteria: 1. *Different visibilities*: the dataset is divided based on the visibility attribute of the objects. Visibility ranges are considered as 0-40%, 40-60%, 60-80%, and 80-100%. 2. *Different object sizes*: the dataset is divided into two groups based on the average object size: objects with a size greater than or equal to 2.5 meters, and objects with a size smaller than 2.5 meters. 3. *Different object distances*: the dataset is split based on different distance ranges, namely 0-20 meters, 20-30 meters, and 30 meters and above. By applying these categorizing and calculations, subsets of data were selected from the clips in the validation dataset to evaluate their performance based on the specified uncertainty conditions.

7 Additional Results

7.1 Detection Results

Metrics. For the 3D detection task, we follow the official evaluation metrics from nuScenes [3], and report nuScenes Detection Score (NDS), mean Average Prediction (mAP), and five True Positive (TP) metrics including mean Average Translation Error (mATE), mean Average Scale Error (mASE), mean Average Orientation Error (mAOE), mean Average Velocity Error (mAVE), mean Average Attribute Error (mAAE).

Detection on nuScenes benchmark. As our UA-Track can jointly optimize tracking and detection, we present the detection results on nuScenes test set and val set in Tab. 7 and Tab. 8 respectively, which demonstrate consistent improvements of our method in the detection task. As a framework design for tracking, our model achieves comparable results (62.7% mAP and 68.0% NDS in the test set) with the concurrent leading detection methods, e.g., HoP and Far3D, and outperforms previous end-to-end detection and tracking model Sparse4D-v3 by a significant margin of 5.7% mAP and 2.4% NDS in the test set.

7.2 Inference Latency

Table 7: Results of 3D detection on nuScenes *test* dataset. † indicates the results obtained from our testing using the provided official model.

Method	Backbone	mAP †	NDS †	mATE †	mASE †	mAOE †	mAVE †	mAAE †
<i>Detection-only</i>								
BEVDet4D [15]	Swin-B	0.451	0.569	0.511	0.241	0.386	0.301	0.121
PETR v2 [31]	V2-99	0.506	0.592	0.536	0.243	0.359	0.349	0.120
BEVDepth [25]	CNX-B	0.520	0.609	0.445	0.243	0.352	0.347	0.127
BEVStereo [24]	V2-99	0.525	0.610	0.431	0.246	0.358	0.357	0.138
SOLOFusion [37]	CNX-B	0.540	0.619	0.453	0.257	0.376	0.276	0.148
AeDet [8]	CNX-B	0.531	0.620	0.439	0.247	0.344	0.292	0.130
StreamPETR [45]	ViT-L	0.620	0.676	0.470	0.241	0.258	0.236	0.134
HoP [58]	ViT-L	0.624	0.685	0.367	0.249	0.353	0.171	0.131
Far3D [17]	ViT-L	0.635	0.687	0.432	0.237	0.278	0.227	0.130
<i>Join Tracking and Detection</i>								
PF-Track-F † [35]	V2-99	0.397	0.387	0.688	0.262	1.800	1.079	0.165
Sparse4D-v3 [29]	V2-99	0.570	0.656	0.412	0.236	0.312	0.210	0.117
UA-Track-F (Ours)	ViT-L	0.627	0.680	0.434	0.237	0.311	0.216	0.130

"F" represent on the full-resolution settings.

We present the inference latency measure in Tab. 9. Our proposed UA-Track, demonstrates greater efficiency compared to previous end-to-end methods, i.e., MUTR3D [55] and DQTrack [23], as our UPD and UQD modules are only applied during the training process.

In comparison to the state-of-the-art PF-Track [35], our UA-Track introduces little additional latency due to the UQI module, and yet this trade-off results in a 5.0% improvement in AMOTA over PF-Track. Further efficiency enhancement in tracking is a promising direction for future research.

Table 9: Inference latency. Frame Per Second (FPS) is evaluated on a single NVIDIA A100 GPU from input images to tracking results.

Method	FPS
PF-Track-S [35]	9.2
DQTrack [23]	6.0
MUTR3D [55]	6.0
UA-Track-S (Ours)	7.5

8 Additional Visualizations

8.1 Qualitative Results of UQI

We present qualitative results of our UQI module in Fig. 7. Our UQI module leverages learned certain priors, i.e., the predicted 2D object location and depth information to formulate initial queries. As shown in Fig. 7, the initial queries generated by our UQI module are accurately positioned within the regions of interest for the objects. This indicates that our module effectively bootstraps latent query states of the objects with reduced uncertainty, leading to improved object localization and tracking results.

Table 8: Results of 3D detection on nuScenes *val* dataset.

Method	Backbone	mAP ↑	NDS ↑	mATE ↓	mASE ↓	mAOE ↓	mAVE ↓	mAAE ↓
<i>Detection-only</i>								
PETR v2 [31]	R101	0.421	0.524	0.681	0.267	0.357	0.377	0.186
BEVDet4D [15]	Swin-B	0.426	0.552	0.560	0.254	0.317	0.289	0.186
BEVDepth [25]	CNX-B	0.462	0.558	0.540	0.254	0.353	0.379	0.200
AeDet [8]	CNX-B	0.483	0.581	0.494	0.261	0.324	0.337	0.195
SOLOFusion [37]	R101	0.483	0.582	0.503	0.264	0.381	0.246	0.207
StreamPETR [45]	R101	0.504	0.592	0.569	0.262	0.315	0.257	0.199
HoP [58]	R101	0.454	0.558	0.565	0.265	0.327	0.337	0.194
Far3D [17]	R101	0.510	0.594	0.551	0.258	0.372	0.238	0.195
<i>Join Tracking and Detection</i>								
MUTR3D [55]	R101	0.349	0.434	–	–	–	–	–
DQTrack [23]	V2-99	0.410	0.503	–	–	–	–	–
PF-Track-F [35]	V2-99	0.399	0.390	0.727	0.268	1.722	0.887	0.211
Sparse4D-v3 [29]	R101	0.537	0.623	0.511	0.255	0.306	0.194	0.192
UA-Track-F (Ours)	ViT-L	0.589	0.655	0.495	0.250	0.249	0.2100	0.1883

"F" represent on the full-resolution settings.

8.2 More Qualitative Results

We provide additional qualitative results in Fig. 8. We compare our UA-Track with the previous state-of-the-art end-to-end tracker, PF-Track [35], on various complex scenarios. In challenging 3D MOT scenarios, characterized by multiple uncertainty factors such as occlusions and small target objects, UA-Track successfully predicts a greater number of tracked bounding boxes with higher localization precision compared to PF-Track [35]. Furthermore, the visualization of our attention scores demonstrates a higher concentration on the center of the objects, indicating that our model pays more attention to the target objects. This observation also highlights the effectiveness of our proposed UPD module with probabilistic attention in modeling the uncertainty associated with the object prediction.

8.3 Video Demo

In addition to the figures, we have also attached a video demo in the supplementary materials, which consists of hundreds of tracking frames that provide a more comprehensive evaluation of our proposed approach.

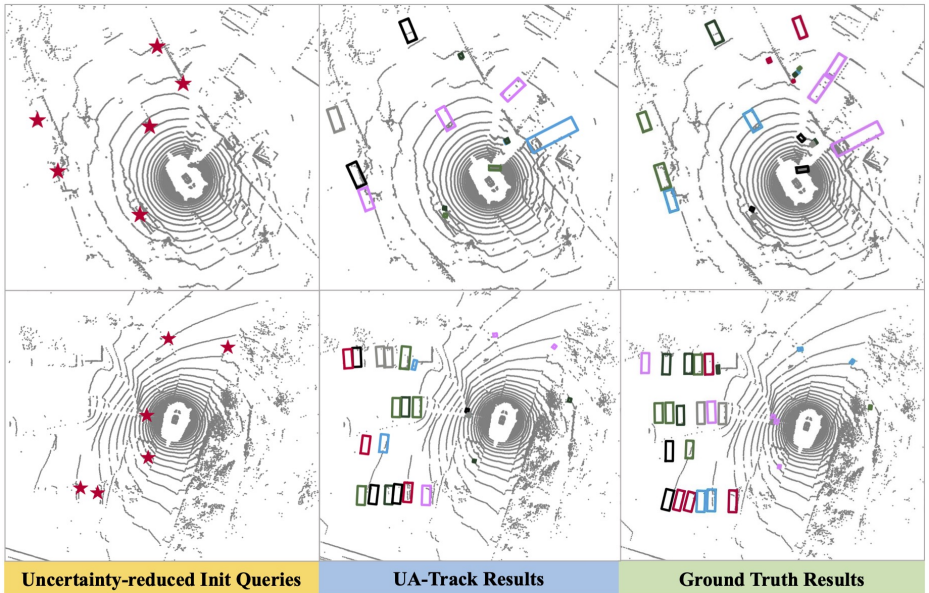


Fig. 7: Qualitative results of our UQI. The initial queries generated by our UQI module accurately locate the regions of interest for the objects, resulting in more accurate tracking results.



Fig. 8: More qualitative results on the nuScenes dataset. The tracking results on several challenging tracking scenarios with uncertainty, including the small size of the target objects and the occlusions. Moreover, we plot the attention scores of object queries, which indicate how strongly the model focuses on the target objects. A higher concentration of color represents a higher attention score and a stronger confidence in the corresponding object.